

Analysis of Fracturing Network Evolution Behaviors in Random Naturally Fractured Rock Blocks

Y. Wang¹ · X. Li¹ · B. Zhang¹

Received: 1 December 2015 / Accepted: 6 June 2016 / Published online: 19 July 2016
© Springer-Verlag Wien 2016

Abstract Shale gas has been discovered in the Upper Triassic Yanchang Formation, Ordos Basin, China. Due to the weak tectonic activities in the shale plays, core observations indicate abundant random non-tectonic micro-fractures in the producing shales. The role of micro-fractures in hydraulic fracturing for shale gas development is currently poorly understood yet potentially critical. In a series of scaled true triaxial laboratory experiments, we investigate the interaction of propagating fracturing network with natural fractures. The influence of dominating factors was studied and analyzed, with an emphasis on non-tectonic fracture density, injection rate, and stress ratio. A new index of P-SRV is proposed to evaluate the fracturing effectiveness. From the test results, three types of fracturing network geometry of radial random net-fractures, partly vertical fracture with random branches, and vertical main fracture with multiple branches were observed. It is suggested from qualitative and quantitative analysis that great micro-fracture density and injection rate tend to maximum the fracturing network; however, it tends to decrease the fracturing network with the increase in horizontal stress ratio. The function fitting results further proved that the injection rate has the most obvious influence on fracturing effectiveness.

Keywords Hydraulic fracturing · Non-tectonic natural fractures · Fracturing network evolution · Sensitive analysis

1 Introduction

In gas shale formations, the discontinuities such as natural fractures (e.g., joints, bedding faces, faults) can have a critical effect on the evolution of the fracturing network. Many shale outcrops, cores, and image logs contain fractures or fracture traces, and microseismic event patterns associated with hydraulic fracture stimulation have also been ascribed to natural fracture reactivation (Warpinski et al. 2009; King 2010; Gale et al. 2014). The key to shale gas production is the presence of natural fractures (Gale and Holder 2008; Jeffrey et al. 2010; Nagel and Sanchez-Nagel 2011; Kresse et al. 2013) and planes of weakness that can result in complex fracture geometries during stimulations. The degree of natural fracture development in a low-matrix-permeability shale reservoir is a controlling factor in gas producibility, since without fractures it is not possible to recover hydrocarbons from these reservoirs. The presence of natural discontinuities alters the way the hydraulic fracture propagates through the rock.

Therefore, the study of the effect of natural fractures on hydraulic fracturing interests many scholars. Many researchers have conducted numerical simulations (Nagel and Sanchez-Nagel 2011; Kresse et al. 2013; Wang et al. 2015a, b), laboratory experiments (Zhou et al. 2008; Bahorich et al. 2012; Hou et al. 2014), and in situ experiments (Tealdi et al. 2008; Suliman et al. 2013) to study the interaction between hydraulic fractures and natural fractures. For their studies, from the origin of natural fractures, the natural fractures belong to a kind of tectonic fractures. Tectonic fractures include shearing fractures, tension-

✉ X. Li
lixiao@mail.iggcas.ac.cn

Y. Wang
good541571889@126.com; wangyu@mail.iggcas.ac.cn

B. Zhang
zhangbo_dzs@126.com

¹ Key Laboratory of Shale Gas and Geoenvironment, Institute of Geology and Geophysics, Chinese Academy of Sciences, No. 19 Beitucheng West Road, Beijing 100029, China

shearing fractures, decollement fractures, bedding fractures, and interbedded fractures (Gale et al. 2014). Tectonic fractures are visible by the naked eye, and they display obvious directivity and regularity in the region; they are usually long extension, and the variation in width is large; the fracture surface is relative smooth and straight; and it usually forms into different fracture sets. However, in China, for typical continental sedimentary shale, taking the Upper Triassic Yanchang Formation of the Ordos Basin for example, the tectonic activities are weak, and faults and folds are not developed in the basin. The proportion of the tectonic fracture is much less than the non-tectonic fractures (Ding et al. 2011; Zhu 2013; Tang et al. 2014). The non-tectonic microfractures (e.g., the diagenetic shrinkage fracture, diagenetic pressolution stitching fracture, overpressured fracture, and thermal shrinkage fracture) are small, high-aspect-ratio cracks in shale formations that result from low differential stresses. This kind of fracture is always irregular, curved, and discontinuous, and has no consistency in different distribution directions. Significant features of non-tectonic fractures are randomly distributed, have a micro-aperture, are not affected by the tectonic field, occur at a small scale, and are present in the majority with micro-fractures (Ding et al. 2003, 2011). These planar or curvilinear openings can provide an opportunity for fluids and/or gases to enter the created cavity. Cement deposits or crack closure may trap fluids or gases, leaving mineral precipitates and a track of enclosed fluids and gases.

During hydraulic fracturing, the stimulation of this type of non-tectonic fractures is also critical to gas producibility (King 2010; Tang et al. 2014). The non-tectonic fractures provide the storage space and flow conduit for oil and gas, and they play a significant role in the fracturing treatment, migration, accumulation, occurrence, and amount of gas in the shale reservoirs. Currently, various studies have been performed on the adsorption, storage capacity, leak-off characteristics, and gas storage capacity of non-tectonic fractures, but the interaction between hydraulic fractures and non-tectonic fractures, and the associated hydraulic fracturing effectiveness has not yet been deeply studied. This paper investigates the effect of non-tectonic fractures on the interaction between hydraulic fractures and microfractures. The influence of dominating factors was studied and analyzed, with an emphasis on non-tectonic fracture density, injection rate, and stress ratio. The study is conducted on sulfoaluminate cement blocks with non-tectonic fracture using laboratory hydraulic fracturing experiments under true triaxial stress conditions.

2 Laboratory Experiment Design

2.1 Scaling of Experiments

Scaling laws are applied to scale hydraulic fracturing parameters in the laboratory to perform a representative field experiment. Scaling laws ensure that the hydraulic fracture is contained within the sample boundaries, and the propagation can be monitored without being affected by the boundary conditions. In the past, scaling laws for performing proper hydraulic fracture experiments were derived (de Pater et al. 1994; Berchenko et al. 2004). These laws scale the experiments in terms of energy rates associated with fluid flow, fracture opening, and rock separation. To have ample time for all measurements, the timescale of fracture propagation is chosen to be approximately 1000 s. In view of the low injection rate in the laboratory, it is necessary to use highly viscous fluids; when using low viscous fluids, we should set high injection rate. Also, we use a material with low fracture toughness for our experiments. When the block has conductive preexisting fractures, another scale factor for the stresses appears, since the fracture aperture depends on the average stress level. For given fracture stiffness, the conductivity will be strongly influenced by the stress level. For instance, in the Barton–Bandis joint model the aperture is given by:

$$U_n = \frac{\sigma_n}{K_{n0}} \frac{1}{\left(1 + \frac{\sigma_n}{K_{n0}U_m^i}\right)} \quad (1)$$

where σ_n is the confining stress, U_m^i is the maximum allowable joint closure at the first load cycle, and K_{n0} is the initial normal stiffness of the discontinuity (Bandis et al. 1985). From this relation, we derive a characteristic stress $\sigma_{n,D}$ that can be used for scaling of the stresses:

$$\sigma_{n,D} = \frac{\sigma_n}{K_{n0}U_m^i} \quad (2)$$

In the absence of preexisting fracture, we perform tests at in situ stresses, but when we introduce a joint, the stress level should also scale with the preexisting fracture stiffness. We chose the applied stress level to ensure open discontinuity in the model block so that we will have the possibility of fluid flow into the preexisting fracture (Bunger 2005; Casas et al. 2006; Sarmadivaleh and Rasouli 2015). Now, we use stresses that are much lower compared with fracture pressure. Therefore, one should be careful in extrapolating the test results to field conditions.

2.2 Model Block Preparation

The cement blocks were prepared in the Rock Mechanics Laboratory at the Institute of Geology and Geophysics, Chinese Academy of Sciences. To represent the physical and mechanical properties of reservoir rock and easy available to prepare the model blocks (Fan and Zhang 2014; Dehghan et al. 2015), artificial cement blocks were generally selected to conduct the experiments. To prepare the testing blocks, cement and quartz sand were mixed in a 1:2 mass ratio. The cement used in this experiment was a kind of quick setting and rapid hardening sulfoaluminate cement no. 425, and the quartz sand corresponds to a 20–40 mesh. The ratio of material to water was 50 %. After uniformly mixed of the cement, sand, and water, the mixture was placed into a 150 mm × 150 mm × 150 mm mold. After the model blocks cured in molds for 2 weeks, they were slowly heated in an oven. They remained in the oven for 2, 4, and 6 h at 200 °C and then were subjected to natural air cooling. Different heating times for the model blocks were used to generate random fractures with different densities. Due to dehydration, shrinkage cracks form, which represents natural non-tectonic random fractures in our model blocks. We drilled the wellbore after the heat treatment to avoid a stress concentration that could influence the shrinkage crack formation. A vertical borehole of 8 mm in diameter was drilled 9 mm deep and parallel to the vertical stress. A metal perforation casing with an inside diameter of 6 mm and spirally distributed perforation holes with a 1 cm height difference and 90° of angular difference between adjacent holes was inserted into the wellbores. The length of the perforation interval was set to 5 cm. Before the heating process, a rock mechanical test and permeability test were also carried out in order to investigate the physical and mechanical parameters of cement blocks (Table 1). After heat treatment of 2, 4, and 6 h for typical blocks, a cylinder-shaped sample with a diameter of 50 mm diameter and a height of 100 mm was drilled from the blocks to measure the mechanical properties. The mechanical properties gradually deteriorated, and the compressive strength decreased with the increasing heat time. When it reached peak stress, the axial strain

Table 1 Physical and mechanical properties of cement blocks before heat treatment

Parameter	Symbol	Value	Units
Uniaxial compressive strength	σ_c	15.37	MPa
Tensile strength	σ_t	1.68	MPa
Elastic modulus	E_0	10.34	MPa
Poisson's ratio	ν	0.28	–
Permeability	K	0.12	mD
Porosity	φ	1.64	%

decreased with the increase in heat time, and this result indicates that the brittleness of the samples increases gradually.

2.3 Experimental Setup

The hydraulic fracturing experiments here were conducted using a true triaxial hydraulic fracturing test system. The test frame of the system has the capacity to apply triaxial stress condition on a 150 mm × 150 mm × 150 mm cubic model block. All of the in situ stress conditions (the vertical, maximum horizontal, and minimum horizontal stresses) are supplied using a hydraulic jack, and the injection pressure is supplied using a servo controlled hydraulic pump of the TAW 2000. The pressure platens are equipped with spherical sheets to ensure equal pressure distribution. Between the model block and the pressure plates, we inserted a thin Teflon sheet covered on both sides with Vaseline to prevent shear stress.

2.4 Experiment Design

During the test, three factors including heat time, injection rate, and stress ratio are considered to investigate the interaction between hydraulic fractures, micro-fractures, and the fracturing network effectiveness. All the experiments were stimulated in a normal-fault region. In this case, the maximum stress was the vertical stress σ_v of 4 MPa, and its value was kept constant for each experiment. The horizontal well was drilled along the direction of vertical stress of σ_v , and its value was 1 MPa. In order to consider a hydraulic fracture field test being simulated in laboratory scale, scaling laws are to be applied to scale the fracturing parameters (de pater et al. 1994; Adachi 2001; Casas et al. 2006). The stress ratio (defined as the ratio of maximum horizontal stress σ_H to minimum horizontal stress σ_h) was 1, 2, and 3, respectively. Therefore, the maximum horizontal stress σ_H equaled to 1, 2, and 3 MPa, respectively. Three injection rates (i.e., 10, 20, and 30 ml/min) were used during the tests. For each experiment, red-dyed water was injected at a constant flow rate (see Table 2). The dye is on-penetrating and therefore highlights the fracture surface generated by the experiment. This can help us observe the fracturing network evolution process easily.

Several indices have been proposed to evaluate the hydraulic fracturing effectiveness, such as the stimulated reservoir area (Hou et al. 2014), leak-off ratio (Wang et al. 2015a), and stimulated DFN length (Wang et al. 2015b). However, the interaction between hydraulic fractures and natural fractures is in three-dimensional space. A concept of the stimulated reservoir volume (SRV) has been proposed to reflect the fracturing effectiveness (Mayerhofer

Table 2 The experimental conditions and results for the hydraulic fracturing tests on random fractured cement blocks

Test	Heat time (H)	Stress ratio	Injection rate (ml/min)	P-SRV
1	2	1	20	0.0683
2	2	3	20	0.0975
3	2	2	10	0.0937
4	2	2	20	0.1091
5	4	1	30	0.1319
6	4	1	10	0.1733
7	4	2	20	0.1443
8	4	1	20	0.1148
9	4	3	10	0.1144
10	6	1	10	0.1547
11	6	2	10	0.1212
12	6	2	20	0.1801
13	6	3	10	0.1054

et al. 2008). Therefore, a better description for the interaction between the random natural fractures and hydraulic fractures, an index of “P-SRV (probability of Stimulated Reservoir Volume),” is proposed to reflect the fracturing effectiveness. The index P-SRV index is defined as the ratio of the total area of fractures per unit volume of model block; it is an index of volumetric intensity. The expression is as follows:

$$P - SRV = \sum_{i=1}^n A_i / V_{\text{block}} \quad (3)$$

where A_i is the area of fracture surface and V_{block} is the volume of model blocks. Figure 1 shows an example of determining the index of P-SRV index.

We kept pumping at a constant flow rate, monitoring as the pressure increased to a maximum value before suddenly decreasing. A sudden decrease in the pressure usually indicates fracture breakdown. We then estimated the fracture volume from the injection rate and pressure to ensure that the fracture was fully developed and still fully contained within the specimen, before ending the experiment by shutting down the pump. Finally, we depressurized the borehole and unloaded the triaxial equipment. After a test, the block was opened with a hammer and chisel, to estimate the total fracture area.

3 Experimental Observations and Results

A sensitivity analysis was conducted over three parameters: the heat time (H), stress ratio (SR), and injection rate (IR).

3.1 General Observations

Figure 2a plots the relationship between pump pressure and injection time. The injection pressure decreases with the increase in heat time; however, the injection time increases with increasing heat time. These results indicate that with short heat time, the brittleness of the model blocks is greater than for blocks with long heat time. Simple bi-planar hydraulic fractures form in this case (specimen No. 4); also, the phenomenon of leak off is the most serious for random fracture developed block (specimen No. 12), and interaction between hydraulic fractures and natural fractures is most obvious for specimen No. 12.

After the test, three types of fracturing network morphology were observed from the studied simulations. They are the radial random net-fractures, the partly vertical fracture with random branches, and the vertical main fracture with multiple branches, as shown in Fig. 2b–d. The injected fluid leaks off to the surface of the specimens. For the reservoir volume reformation, the more complex the fracture morphology, the better the fracturing effectiveness is. Therefore, the radial random net-fractures represent a promising fracturing network.

3.2 Effect of Heat Time on Fracturing Network Evolution

The density of natural fractures is crucial to the overall response (e.g., microseismicity activities, SRV, well production). Currently, after the literature review, almost all of the work is focused on the influence of tectonic natural fractures on hydraulic fracturing.

The duration of heat time here can reflect the density of non-tectonic fractures in model blocks. Generally, the longer the heat time, the much more intense of the random fractures are. For specimens with a long heat time, the model block is seriously damaged, and the mechanical strength of the material is relatively low. The initiation and propagation of hydraulic fracturing is easier than specimens with a short heat time. In addition, non-tectonic fractures are much more evenly distributed on specimens with a long heat time, and the interaction between hydraulic fracture and non-tectonic natural fracture is stronger. In this case, the fracturing network effectiveness is better. Taking the specimens Nos. 2 (2 h), 7 (4 h), and 12 (6 h) for example, the fracturing effectiveness gets better with the increase in heat time, as shown in Fig. 3. Two types of fracturing network morphology of partly vertical fracture with random branches and radial random net-fractures were observed. The number of fractures on the main fracture plane increases with the increasing heating time; it is 3, 4, and 13, respectively. These results indicate

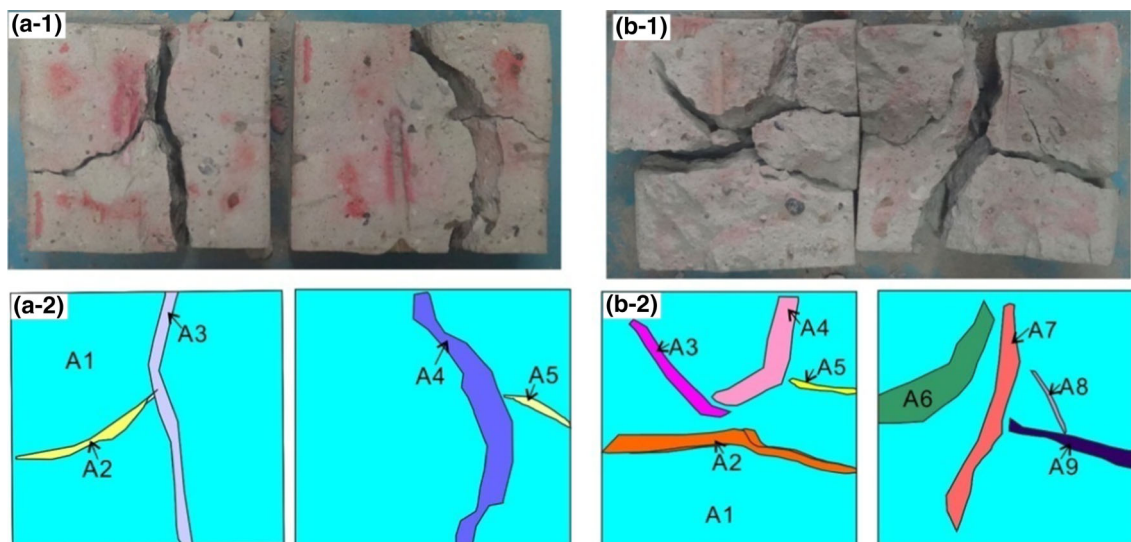


Fig. 1 Determination of the index P-SRV index for specimen Nos. 12 (a) and 8 (b). P-SRV is equal to the ratio of the total fracture surface area to the volume of the model blocks

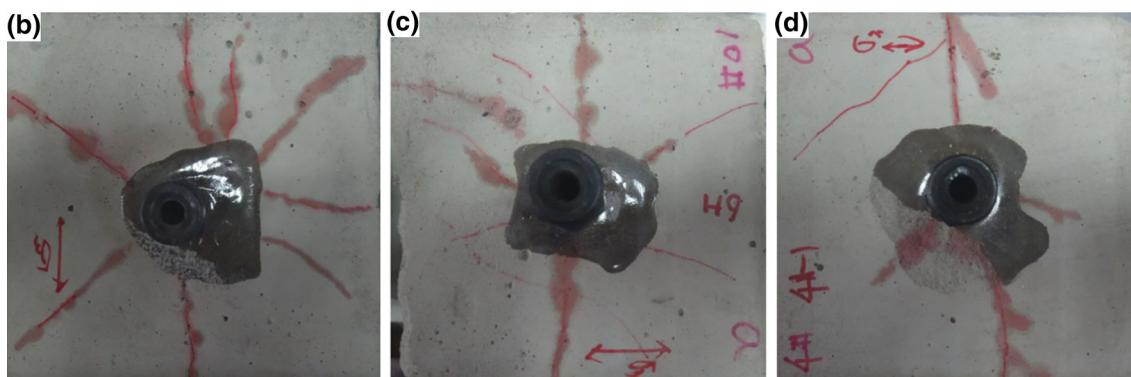
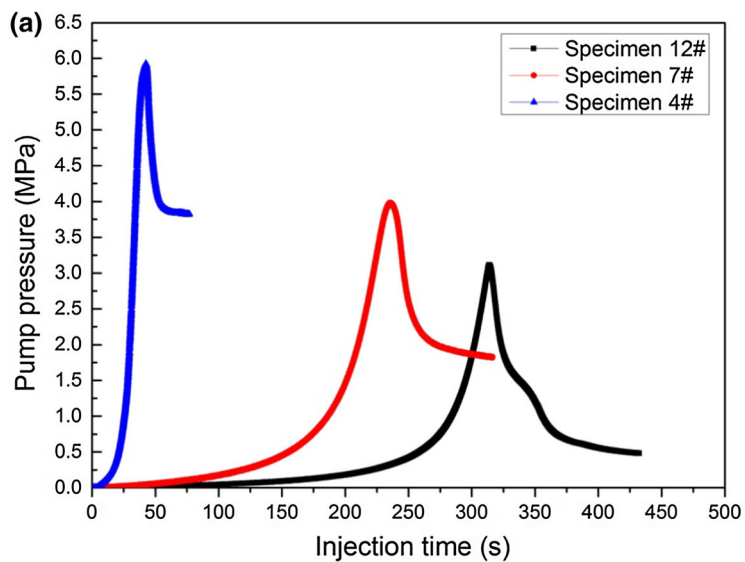


Fig. 2 Observed three typical kinds of network morphology. **a** is the relationship between pump pressure and injection rate for specimen Nos. 12, 7, and 4; **b** is the radial random net-fractures for specimen

No. 12; **c** is the partly vertical fracture with random branches for specimen No. 7; and **d** is the vertical main fracture with multiple branches for specimen No. 4

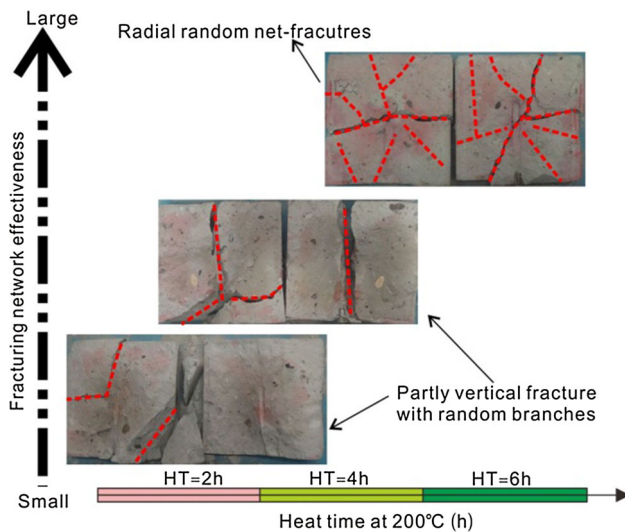


Fig. 3 Geometry of fracturing network for experimental models with different heat times, P-SRV is strongly related to heat time. The relationship between fracturing network effectiveness and heat time, for example, specimen Nos. 4 (2 h), 7 (4 h), and 12 (6 h) for example

that the density of non-tectonic fractures in gas shale formations has a significant effect on the fracturing network effectiveness. The key to shale gas production is the presence of natural fractures (King 2010; Palmer and Moschovidis 2010) and planes of weakness that can result in complex fracture geometries during stimulations. Taking the specimen Nos. 4, 7, and 12 for example, the injection rate is 20 ml/min, stress ratio is 2, and the relationship between index P-SRV and heating time is shown in Fig. 4. The relationship follows a linear function, and the correlation coefficients are both greater than 95%. The fracturing effectiveness increases with the increase in natural fractures.

3.3 Effect of Stress Ratio on Fracturing Network Evolution

The in situ stress contrasts obviously have the most significant effect on fracture height growth. The importance of in situ field stress was recognized early in 1961 (Perkins and Kern 1961) and has been extensively studied in modeling (e.g., Simonson et al. 1978; Voegele et al. 1983; Zhou et al. 2010), mineback tests (Warpinski et al. 1982), and numerous laboratory experiments. But few reports about how the stress contrast affects the shear stimulation were reported. Stress ratio also plays an important role in the generation of the fracturing network. Therefore, the primary interest in simulating the sensitivity of the stress ratio is to obtain a better understanding of how output is affected by it. Taking the specimen Nos. 10 (SR = 1), 11 (SR = 2), and 13 (SR = 3) for example, Fig. 5 shows the results of

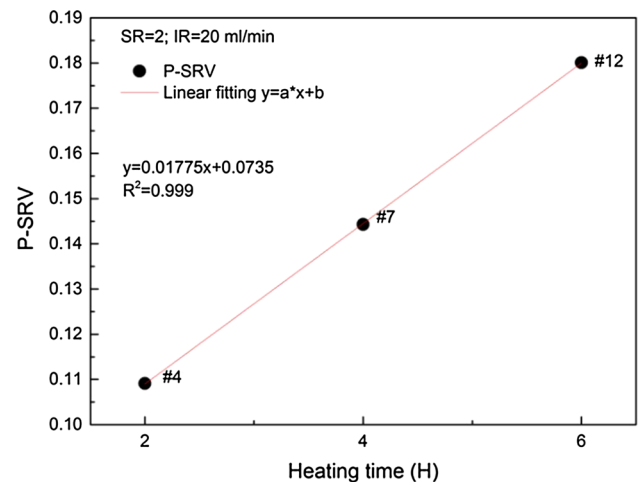


Fig. 4 Plot of index P-SRV against heating time, relationship of them follows linear equation with good correlation. For the studied cases, the stress ratio is 2, and the injection rate is 20 ml/min

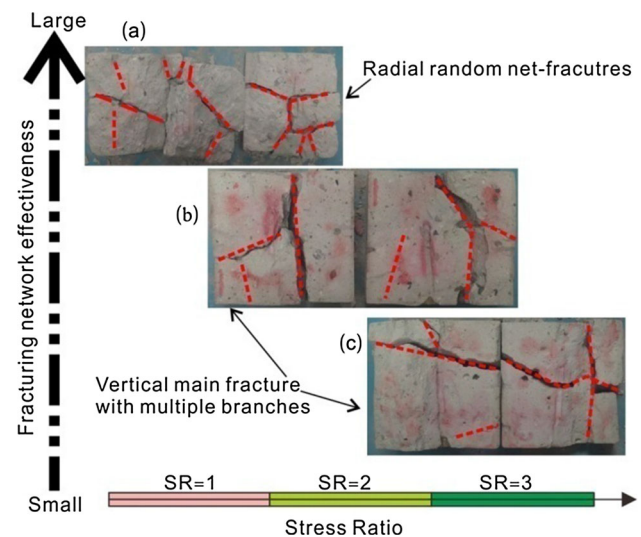


Fig. 5 Geometry of the fracturing network for experimental models with different stress ratios. The morphology of hydraulic fractures is strongly related to the stress ratio. In this case, taking specimen Nos. 10, 11, and 13 (6 h) for example, the stress ratio of them is 1, 2, and 3, respectively

fracture stimulated morphology with a stress ratio of 1, 2, and 3, respectively. With different stress ratios, the morphology of the fracturing network is different. Two types of fracturing network geometries were observed. At a low stress ratio, the radial random net-fractures dominated the geometry of the hydraulic fracture; at stress ratios equal to 2 and 3, a vertical main fracture with multiple branches were observed. In addition, the number of fractures on the main fracture surface decreases with the increase in stress ratio; there are 15, 7, and 6, respectively. The relationship between P-SVR and stress ratio is shown in Fig. 6, and they follow a linear fitting function with good correlation.

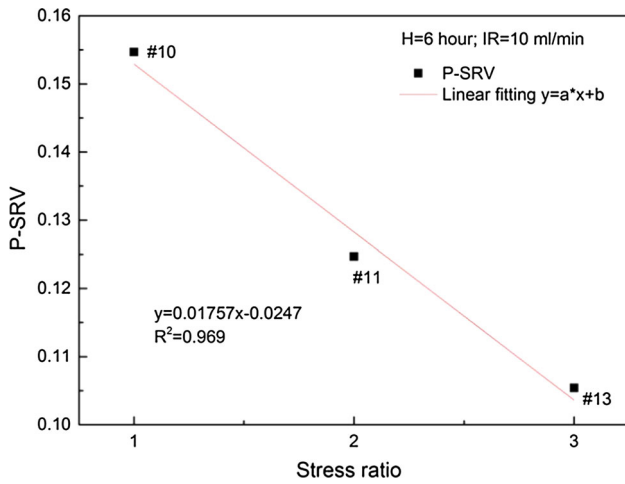


Fig. 6 Plot of index P-SRV against stress ratio, relationship of them follows linear function with good correlation. For the studied cases, the heating time is 6 h, and the injection rate is 10 ml/min

3.4 Effect of Injection Rate on Fracturing Network Evolution

The injection rate and injection pressure along with the viscosity of the injected fluid are the operational parameters that can be used to effectively design hydraulic fracturing. The slick-water fluid with minimum viscosity has evolved to increase the formation-face contact of the fracture system in a very small area of reservoirs by opening the natural fractures (King 2010; Kresse et al. 2013). Therefore, the water-frac fluid is used to stimulate the random natural fractures. Figure 7 shows the geometry morphology of specimen Nos. 6 (Fig. 7a), 5 (Fig. 7b), and 8 (Fig. 7c), respectively. As shown, the number of fractures on the main fracture surface increases with increasing injection rate, and the number is 5, 7, and 11, respectively. From the result of relationship between P-SRV and injection rate, they follow an exponential function with good correlation, as shown in Fig. 8.

Three types of fracturing network geometries were observed, with an increasing injection rate: the changes of geometry are from the vertical main fracture with multiple branches, the partly vertical fracture with random branches, to radial random net-fractures. These results indicate that the higher the injection rate, a higher injection pressure is applied, and the better hydraulic fracturing effectiveness can be obtained. The quantitative analysis results further prove that a high injection rate is good to form a complex fracturing network. This conclusion is consistent with the results of King (2010) and Nagel and Sanchez-Nagel (2011). At a low injection rate, the fracturing fluid usually flows along non-tectonic random fractures and bedding faces. With an increased injection rate, free deviation of the injected fluid from the maximum horizontal direction becomes very easy for hydraulic fractures. The hydraulic

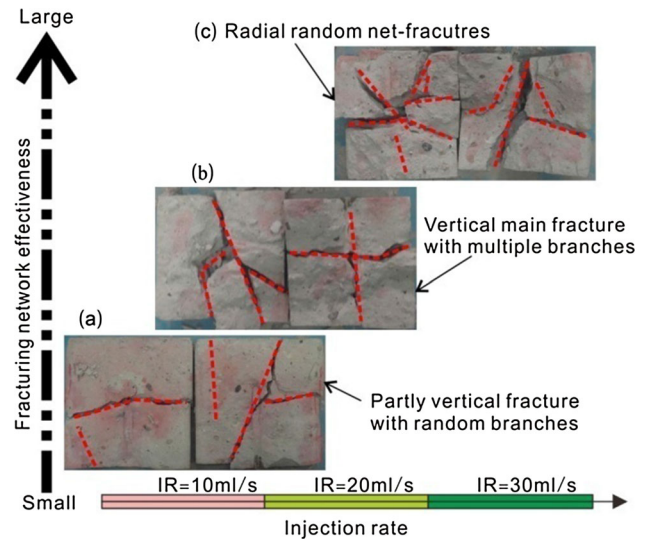


Fig. 7 Geometry of the fracturing network for experimental models with different injection rates, the morphology of hydraulic fractures is strongly related to the injection rate. In this case, taking specimen Nos. 6, 5 and 8 for example, the injection rate for each is 10, 20, and 30 ml/s, respectively

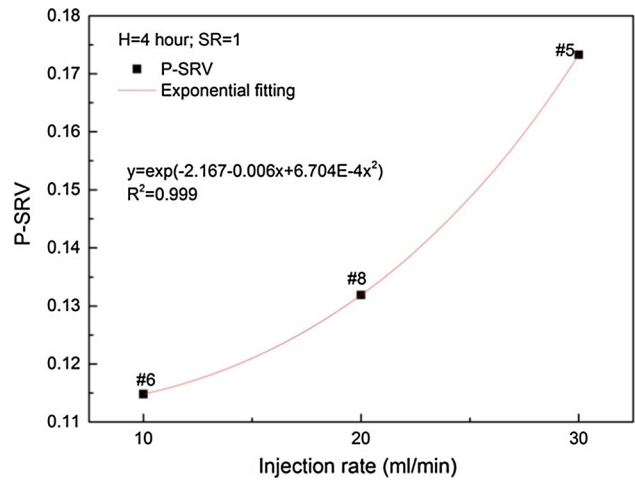


Fig. 8 Plot of index P-SRV against injection rate, relationship of them follows exponential function with good correlation. For the studied cases, the heating time is 4 h, and the stress ratio is 1

fractures can communicate natural fractures and greatly increases the simulated reservoir volume. At a high injection rate, radial random net-fractures are easy to form, and the associate fracturing network is the most complicated, when using the water-frac treatment in this work.

4 Discussions

Various scholars have conducted a series of experiments to study the interaction between natural fractures and hydraulic fractures. Zhou et al. (2010) performed

laboratory experiment to investigate the influence of a random natural fracture system on geometry and propagation behaviors of hydraulic fractures. The hydraulic fracture tended to be a dominating fracture with random multiple branches with a high difference of horizontal stresses. Our test result is consistent with the results of Zhou et al. (2010). It should be mentioned that they have only considered the effect of the stress ratio on the interaction between natural fractures and induced fractures. By numerical simulation, some authors also found that the density of natural fractures, and also the injection rate is important to well production (Nagel and Sanchez-Nagel 2011; Wang et al. 2015b). However, the study on multi-factor analysis that affects the fracturing effectiveness is discussed here. For the studied three factors, laboratory experiments indicated that three types of fracture network are observed. In this work, using the water-frac treatment, the specimens with a low stress ratio, a high non-tectonic fracture density, and a high injection rate are prone to form radial random net-fracture; the fracturing effectiveness is the best in this case.

As for non-tectonic natural fractures, due to randomly distributed, irregular, and discontinuous, the morphology of the fracturing network is different from that of tectonic natural fractures. It was observed that with the increase in stress ratio, hydraulic fractures propagate along and across the natural fracture; it is different to turn direction at the tips of natural fracture. For a tectonic natural fracture that developed a rock block, experimental results indicated three interaction modes of fractures at interaction points with pre-fractures: crossing, opening, and shear slippage of the preexisting fracture (Dehghan et al. 2015). However, for the non-tectonic fracture developed model blocks, in some cases, the hydraulic fracture was either propagated from the fracture tip along the direction of maximum horizontal stress or propagated across the preexisting fracture in the normal stress regime after interaction and opening of the pre-fracture.

5 Conclusions

Laboratory experiments on synthetic model blocks with non-tectonic fractures were conducted to investigate the influence of fracture density, stress ratio, and injection rate on fracturing network evolution.

The results of this research study indicated that hydraulic fracture geometry was a simple, bi-wing, plane fracture before interaction with natural fractures, but after interaction with non-tectonic fractures, its geometry was affected by the stress ratio, injection rate, and fracture density. Three types of complex fracturing network geometry are observed during hydraulic fracturing, and

they are the radial random net-fractures, the partly vertical fracture with random branches, and the vertical main fracture with multiple branches. It was also clear that the applied stress had distinctly different effects on the fracturing network geometry.

The stress ratio was shown to alter both the extent and morphology of the sheared natural fractures. A smaller volume of formation experiences stimulation along the natural fractures with an increase in stress ratio. The morphology of fracturing is strongly affected by the stress ratio. Experimental results demonstrated that the fracturing network was complex at low in situ stress regions with a high operational injection rate. With increasing injection rate, the morphology of the fracturing network is different. At high injection rate, the radial random net-fractures are observed around the wellbore, and the fracturing effectiveness is better than the results from low injection rate. From the curve fitting results, a linear negative correlation and positive correlation between stress ratio and heating time are obtained, respectively. However, an exponential correlation is obtained from the link between injection rate and fracturing effectiveness. These results further indicate that the injection rate plays a critical role in distributing the fluid between the hydraulic fractures and the natural fractures.

Acknowledgments The authors would like to thank the editors and the anonymous reviewers for their helpful and constructive comments. This work was supported by the Beijing National Science Foundation of China (Grants No. 8164070), National Natural Science Foundation of China (Grants Nos. 41330643, 41502294), China Postdoctoral Science Foundation Funded Project (Grants No. 2015M571118), and the Strategic Priority Research Program of the Chinese Academy of Sciences (Grants Nos. XDB10030000, XDB10030300, and XDB10050400).

References

- Adachi JI (2001) Fluid-driven fracture in impermeable and permeable rock, PhD Dissertation, University of Minnesota
- Bahorich B, Olson JE, Holder J (2012) Examining the effect of cemented natural fractures on hydraulic fracture propagation in hydrostone block experiments. *SPE* 160197
- Berchenko I, Detournay E, Chandler N, Martino J (2004) An in situ thermo-hydraulic experiment in a saturated granite I: design and results. *Int J Rock Mech Min Sci* 41(8):1377–1394
- Bunger A (2005) Near-surface hydraulic fracture. Ph.D. dissertation, University of Minnesota, Minneapolis, USA
- Casas L, Miskimins JL, Black A, Green S (2006) Laboratory hydraulic fracturing test on a rock with artificial discontinuities. *SPE paper no. 103617-MS*, PE annual technical conference and exhibition, 24–27 September, San Antonio, TX, USA
- de Pater CJ, Cleary MP, Quinn TS, Barr DT, Johnson DE, Weijers L (1994) Experimental verification of dimensional analysis for hydraulic fracturing. *SPE Prod Facil* 9(4):230–238
- Dehghan AN, Goshtasbi K, Ka Ahangari, Jin Y (2015) The effect of natural fracture dip and strike on hydraulic fracture propagation. *Int J Rock Mech Min Sci* 75:210–215

- Ding WL, Zhang BW, Li TM (2003) Formation of non-tectonic fractures in mudstones in Gulong depression. *Oil Gas Geol* 24:50–54
- Ding WL, Xu CC, Jiu K (2011) The research process of shale fracture. *Adv Earth Sci* 2:135–145
- Fan TG, Zhang GQ (2014) Laboratory investigation of hydraulic fracture networks in formations with continuous orthogonal fractures. *Energy* 79:1–10
- Gale JFW, Holder J (2008) Natural fractures in the Barnett shale: constraints on spatial organization and tensile strength with implications for hydraulic fracture treatment in shale-gas reservoirs: the 42nd U.S. rock mechanics symposium (USRMS), San Francisco, CA, June 29–July 2
- Gale JFW, Laubach SE, Olson JE, Eichhubl P, Fall A (2014) Natural fractures in shale: a review and new observations. *AAPG Bull* 98:2165–2216
- Hou B, Chen M, Li ZM, Wang YH, Diao C (2014) Propagation area evaluation of hydraulic fracture networks in shale gas reservoirs. *Petrol Explor Dev* 41(6):833–838
- Jeffrey RG, Zhang X, Bungler AP (2010) Hydraulic fracturing of naturally fractured reservoirs. In: *Proceedings of the 35th workshop on geothermal reservoir engineering*, Stanford, CA, USA, 1–3 February
- King GE (2010) Thirty years of gas shale fracturing: What have we learned? Paper SPE 133456 presented at the SPE annual technical conference and exhibition, Florence, Italy, 19–22 September
- Kresse O, Weng XW, Gu HR, Wu RT (2013) Numerical modeling of hydraulic fractures interaction in complex naturally fractured formations. *Rock Mech Rock Eng* 46:555–568
- Mayerhofer MJ, Lonon EP, Warpinski NR, Cipolla CL, Walser D, Rightmire CM (2008) What is stimulated rock volume (SRV)? In: SPE 119890, presented at the 2008 SPE shale gas production conference, Fort Worth, TX, November 16–18, 2008
- Nagel N, Sanchez-Nagel M (2011) Stress shadowing and microseismic events: a numerical evaluation. Paper SPE 147363 presented at the SPE annual technical conference and exhibition, Denver, CO, USA, 30 October–2 November. SPE 152192
- Palmer I, Moschovidis Z (2010) New method to diagnose and improve shale gas completions, Paper SPE 134669 presented at the SPE annual technical conference and exhibition, Florence, Italy, 2010, 19–22 September
- Perkins TK, Kern LR (1961) Widths of hydraulic fractures. *JPT* 13:937–949
- Sarmadivaleh M, Rasouli V (2015) Test design and sample preparation procedure for experimental investigation of hydraulic fracturing interaction modes. *Rock Mech Rock Eng* 48(1):93–105
- Simonson ER, Abou-Sayed AS, Clifton JJ (1978) Containment of massive hydraulic fractures. *SPE J* 18:27–32
- Suliman B, Meek R, Hull R, Bello H, Portis D, Richmond P (2013) Variable stimulated reservoir volume (SRV) simulation: eagle ford shale case study. Paper SPE 1582601 presented at the unconventional resources technology conference held in Denver, CO, USA, 12–14 August
- Tang X, Zhang JC, Wang XZ (2014) Shale characteristics in the southeastern Ordos Basin, China: implications for hydrocarbon accumulation conditions and the potential of continental shales. *Int J Coal Geol* 128:32–46
- Tealdi L, Obondoko D, Isella D, Baldini D, Baioni A, Okassa F, Pace G (2008) The kitina mature offshore field rejuvenation: massive multistage hydraulic fracturing, long reach wells, improved oil recovery techniques. The paper was prepared for presentation at the 2008 SPE Europec/EAGE annual conference and exhibition held in Rome, Italy, 9–12 June 2008, SPE 113609
- Voegele MD, Abou-Sayed AS, Jones AH (1983) Optimization of stimulation design through the use of in situ stress determination. *JPT* 35:1071–1081
- Wang Y, Li X, Zhou RQ, Tang CA (2015a) Numerical evaluation of the shear stimulation effect in naturally fractured formations. *Sci China Earth Sci* 58:1–6. doi:10.1007/s11430-015-5204-5
- Wang Y, Li X, Zhou RQ, Zheng B, Zhang B, Wu YF (2015b) Numerical evaluation of the effect of fracture network connectivity in naturally fractured shale based on FSD model. *Sci China Earth Sci* 58:1–14. doi:10.1007/s11430-015-5164-9
- Warpinski NR, Fnley SJ, Vollendorf WC (1982) The interface test series: an in situ study of factors affecting the containment of hydraulic fractures. Sandia National Laboratories Report, SAND, pp 2381–2408
- Warpinski NR, Waltman CK, Du J (2009) Anisotropy effects in microseismic monitoring. Paper SPE 124208, presented at the 2009 SPE annual meeting and exhibition, New Orleans, LA, USA, 4–7 October
- Zhou J, Chen M, Jin Y, Zhang GQ (2008) Analysis of fracture propagation behavior and fracture geometry using a tri-axial fracturing system in naturally fractured reservoirs. *Int J Rock Mech Min Sci* 45:1143–1152
- Zhou J, Jin Y, Chen M (2010) Experimental investigation of hydraulic fracturing in random naturally fractured blocks. *Int J Rock Mech Min Sci* 47:1193–1199
- Zhu DW (2013) Developmental characteristics, major regulating factors and distribution prediction of fractures in shale of upper triassic Yangchang formation in Yangchang oil–gas field. China University of Geosciences for Master Degree, pp 45–53